

# Amorphous phase separation of ionomer glasses

A. RAFFERTY, R. HILL

*Department of Materials Science and Technology, University of Limerick, Limerick, Ireland*  
E-mail: Robert.Hill@UL.IE

D. WOOD

*Division of Restorative Dentistry, Leeds Dental Institute, University of Leeds, Clarendon Way, Leeds LS2 9LU, UK*

Ionomer glasses of generic composition  $\text{SiO}_2\text{-Al}_2\text{O}_3\text{-P}_2\text{O}_5\text{-CaO-CaF}_2$  were studied using differential scanning calorimetry (DSC) and high temperature dynamic-mechanical thermal analysis (DMTA). High temperature DMTA was used to measure the glass transition temperatures ( $T_g$ ) of the original starting glass compositions, as well as being able to follow amorphous phase separation (APS) within the glass. High temperature DMTA traces of all the glasses studied exhibited two maxima in  $\tan \delta$ . These maxima correspond to two glass transition temperatures and demonstrate that amorphous phase separation of the parent glass into two glass phases had occurred. A DMTA study of a Sodium-Boro-Silicate glass, which is known to undergo amorphous phase separation yielded similar results. DSC studies showed that the ionomer glasses underwent a nucleation process at temperatures just above the glass transition temperature which is probably associated with APS. The glasses exhibited optimum nucleation temperatures which moved to lower temperatures with longer hold times indicating the time dependency of the APS process.

© 2000 Kluwer Academic Publishers

## 1. Introduction

The phenomenon of amorphous phase separation in glasses has since about 1950 become an important topic of modern glass research [1]. It has been the subject of many investigations and there is a whole area of glass science devoted to this phenomenon in different glass-forming systems [2]. This particular study will concentrate on the phenomenon as it effects ionomer glasses and also a sodium-boro-silicate glass composition.

A homogeneous single phase will separate into two or more phases of different compositions if the free energy of the system with two or more distinct phases is lower than that of the system with one single homogeneous phase [3]. Many glasses exhibit amorphous phase separation prior to crystal nucleation and growth during the heat treatment schedule required to convert them to glass-ceramics. It is well known that such separation may aid subsequent crystallisation by producing a phase with a greater tendency to nucleate than the initial glass [4]. Phase separation which occurs above the liquidus is known as stable immiscibility, whereas phase separation at temperatures below the liquidus is known as metastable immiscibility. It is metastable immiscibility that is primarily of importance in this study. For a review of APS in relation to subsequent crystal nucleation the reader is referred to James [4], as well as a comprehensive general review of APS in inorganic glasses [5].

Perhaps the earliest practical application of phase separation was that of Hood and Nordberg who developed the Vycor process for the production of high

silica ware by a porous glass route [2]. A range of compositions in the  $\text{R}_2\text{O-B}_2\text{O}_3\text{-SiO}_2$  system, where  $\text{R} = \text{Na, K or Li}$ , exhibit phase separation when suitably heat-treated, with each phase being continuous. Subsequent removal of the soluble alkali-borate phase by acid leaching results in a highly siliceous (>95%) skeleton with a mutually interconnected pore structure. Thermal heat-treatment of Vycor-type glasses has a very strong influence on the phase separation process and hence the pore size distribution and morphology of the leached glass network. The tendency for borosilicate glasses to phase separate can be controlled by the addition of small quantities of other elements into the glass. Small additions of  $\text{Al}_2\text{O}_3$  are known to retard the separation process [2].

Phase separation in ionomer glasses has been less extensively studied. Ionomer glasses generally contain 20–36%  $\text{SiO}_2$ , 15–40%  $\text{Al}_2\text{O}_3$ , 0–35%  $\text{CaO}$ , 0–10%  $\text{AlPO}_4$ , 0–40%  $\text{CaF}_2$ , 0–5%  $\text{Na}_3\text{AlF}_6$  and 0–6%  $\text{AlF}_3$ . These glasses have been the subject of much research into improving glasses for use in glass-polyalkenoate cements, which are used in restorative dentistry [6]. Most commercial glass-ceramic systems utilise prior amorphous phase separation to ensure homogeneous nucleation and produce a rapidly nucleating glass ceramic. An example of this is the development of Dicot<sup>TM</sup> by Grossman and co-workers [7, 8] which was the first castable glass-ceramic for dental use. Ionomer glasses and fluoro-phospho-silicate glasses, like the borosilicate glass system, undergo APS. Additions of fluorine increase the disruption of the glass network by

replacing bridging oxygens by non-bridging fluorines [9]. Small amounts of  $P_2O_5$  are also known to influence crystalline nucleation rates strongly [10]. McMillan and Partridge [11] found that quite small concentrations of  $P_2O_5$  are effective in inducing the desired amorphous phase separation necessary for nucleation in a wide range of glass compositions derived from the  $Li_2O-Al_2O_3-SiO_2$ ,  $Li_2O-MgO-SiO_2$  and  $MgO-Al_2O_3-SiO_2$  systems. Confirmation that  $P_2O_5$  enhances phase separation in  $Li_2O-SiO_2$  glasses was provided by the work of Tomozowa [12].

Barry *et al.* [13] observed phase separation of ionomer glasses into two phases; one of which is more susceptible to acid attack. The extent and scale of any phase separation will clearly effect the susceptibility of the glass to acid attack. Indeed, Hill and Wilson [14] have shown there is a quite marked effect in both appearance of the glass and the properties of the glass ionomer cement as a result of phase separation. They studied glasses based on the generic formula  $SiO_2-Al_2O_3-CaF_2-CaO$ . They describe the phase separated droplets as consisting of a central core of fluorite surrounded by an amorphous region, which is readily etched by acid, a less readily etched subsurface layer, and an outer layer which is rapidly etched. Hill and Wilson [14] maintain that the amorphous region of the droplet is enriched in calcium and fluoride and depleted in aluminium and silicon. The crystalline component consists only of calcium and fluoride, whilst the matrix surrounding the droplet is enriched in aluminium and silicon and depleted in calcium and fluoride.

The evidence for the existence of APS is generally provided by transmission electron microscopy (TEM) [1]. Another powerful technique for investigating the early stage kinetics of phase separation is small angle x-ray scattering (SAXS) [10]. A novel alternative to TEM and SAXS as a means of studying APS is high temperature dynamic mechanical thermal analysis. High temperature DMTA is a sensitive technique for determining glass transition temperatures, each of which give rise to a pronounced damping peak. This contrasts sharply with the more conventional DTA and DSC techniques, where the  $T_g$  appears as a subtle change in slope in the plot of heat flux against temperature, which is difficult to determine accurately. As APS results in the formation of two or more amorphous phases, it follows that a phase separated glass should exhibit at least two glass transition temperatures. To date, low temperature dynamic mechanical thermal analysis has been used almost exclusively to study ion hopping motions in inorganic glasses [15]. Douglas [16] recognised the potential of high temperature DMTA for looking at non-bridging oxygen rotations and network motion. More recently, Stevels [17] has emphasised the advantages of studying network motions using this technique. DMTA experiments on inorganic oxide glasses looking at the network motions that correspond to  $T_g$  are still scarce. Only in two published papers is there multi-frequency data over the glass transition region [18–20]. Hill and Gilbert [21] studied the  $Li_2O-ZnO-SiO_2$  glass-ceramic system. Sharp loss peaks corresponding to two glass transition temperatures were observed in these glasses.

TABLE I Glass compositions studied in molar proportions

Glass	SiO <sub>2</sub>	Al <sub>2</sub> O <sub>3</sub>	P <sub>2</sub> O <sub>5</sub>	CaO	CaF <sub>2</sub>	Ca/P Ratio	Melt Temperature/°C
1	4.5	3	1.6	3	2	1.40	1420
2	4.5	3	1.4	3	2	1.61	1420
3	4.5	3	1.5	3.5	1.5	1.67	1430

An increase in the storage modulus was observed as the glasses crystallised. The much greater sensitivity of DMTA over conventional DSC and DTA techniques was clearly demonstrated by the ability to detect two previously unobserved transitions in the crystallised glass-ceramics.

## 2. Experimental procedures

### 2.1. Preparation of glass samples

Ionomer glasses were synthesised, each of which contained the five components;  $SiO_2$ ,  $Al_2O_3$ ,  $P_2O_5$ ,  $CaO$  and  $CaF_2$ . Table I shows the compositions of the three glasses along with their respective firing temperatures and calcium phosphate (Ca/P) ratios.

A fourth Vycor glass was also synthesised. This was a Sodium-Boro-Silicate glass containing 51.5 wt. %  $SiO_2$ , 40 wt. %  $B_2O_3$  and 8.5 wt. %  $Na_2O$  which was produced in accordance with a composition chosen from a patent by Hammel *et al.* [22]. This glass is well known to phase separate into a silica-rich and a borate-rich phase upon suitable heat-treatment. The borate-rich phase can then be leached with water and then acid to form a microporous glass.

Glasses 1 and 2 are of the same series but differ in that glass 1 has a larger quantity of phosphate than glass 2. Glass 3 is of a different series and has a Ca/P ratio of 5 : 3. This is the ratio of calcium to phosphate in the apatite crystalline phase ( $Ca_5(PO_4)_3F$ ). Both series contain a basic oxide in the form of  $CaO$ . This basic oxide helps eliminate silicon tetrafluoride loss from the melt during firing [23]. In all these glasses there is also sufficient  $Ca^{2+}$  ions to charge balance the  $Al^{3+}$  ions present and allow them to occupy a tetrahedral role within the glass network [24].

All the glasses were prepared by melting appropriate amounts of the different glass reagents in lidded high density mullite crucibles (Zedmark Refractories, Earlsheaton, Dewsbury, UK) at 1420°C for 120 minutes. The resulting glass melts were then shock quenched directly into water to produce frit. The glass frit was then ground and sieved to particle size fractions of  $>45 \mu m$  to  $<150 \mu m$  for DSC analysis. Glass bars were produced for dynamic mechanical thermal analysis. This was done by recasting glass frit in alumina crucibles (VZS Technical Ceramics, Glenroites, Fife, Scotland) and pouring onto a pre-heated sheet of steel. The cast bars of glass were then annealed for 240 minutes at 50°C below the glass transition temperature. Bars measuring approximately  $6 \times 2 \times 30$  mm were cut from this annealed glass using a diamond edged flitting wheel. This allowed almost perfectly flat samples to be produced which is vital for successful performance of the DMTA. The edges of the

samples were then ground down and polished to a 1  $\mu\text{m}$  finish to remove surface cracks. A number of these bars were also heat-treated in an Austromat 3001 Dental Porcelain Furnace (Austromat®-Keramikofen, D-83395 Freilassing, Germany) at their optimum nucleation temperatures and further DMTA runs carried out in order to assess the effect, if any of pre-heat-treating the glass above its glass transition temperature.

## 2.2. High temperature DMTA analysis

High Temperature Dynamic Mechanical Thermal Analysis is an extremely powerful technique for investigating APS in glasses. It can be used to examine three major types of motion in inorganic glasses, the most important of which are network motions associated with the glass transition temperature. DMTA involves the application to a material of an oscillating stress. If the material is perfectly elastic, the deformation and hence the strain occur exactly in phase with the applied stress. If perfectly viscous, the strain will be exactly 90° out of phase. However, when some internal molecular motion is occurring in the same frequency range as the applied stress, the material exhibits viscoelastic behaviour and the strain response will lag behind the applied stress by some phase angle  $\delta$ . This phase lag results from the time necessary for molecular rearrangements and is associated with relaxation phenomena. The phase angle  $\delta$  is given by:

$$\tan \delta = \frac{E''}{E'} \quad (1)$$

The real part of the modulus,  $E'$  is called the storage modulus. This is because it is related to the storage of energy as potential energy and its release in the periodic deformation. The imaginary part,  $E''$  is the loss modulus and is associated with the dissipation of energy as heat when the material is deformed. The loss tangent  $\delta$  is also called the internal friction, or damping, and is the ratio of energy dissipated per cycle to the maximum potential energy stored during a cycle. By studying these parameters as a function of temperature and frequency for a given material, it is possible to study molecular motions. For a thorough review of the principles of DMTA the reader is referred to a paper by Hill *et al.* [21].

The apparatus used was a Polymer Laboratories High Temperature DMTA (Thermal Sciences Division, Loughborough, U.K.), with a maximum furnace head temperature of 800°C. The DMTA apparatus consists of a mechanical spectrometer head which is surrounded by a demountable temperature enclosure. This is interfaced with both a dynamic control system/analyser and a temperature programmer. The sample is held in the apparatus by means of a single cantilever clamp as shown in Fig. 1.

While held rigid at one end, the sample is clamped between two knife edges, one of which is attached to the end of a ceramic drive shaft. This part of the apparatus is isolated in the temperature-controlled furnace by means of a large ceramic baffle. The brittle nature of the glass specimens meant that the imposed strain

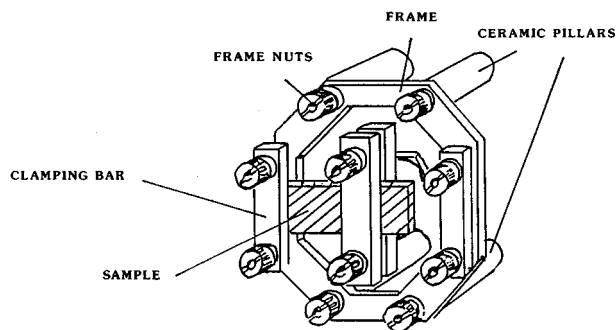


Figure 1 A single cantilever clamp.

was kept low. The strain chosen gave a nominal peak-to-peak displacement of 10  $\mu\text{m}$  though much larger strains than this can be used if required. Samples were run in the single frequency mode at 1 Hz while heating at 5°C/min.

## 2.3. Thermal analysis

Differential Scanning Calorimetry (DSC) was used to examine thermal transitions in these glasses. Using a Stanton-Redcroft DSC 1500 instrument (Rheometric Scientific, Epsom, UK), values were obtained for the glass transition temperature ( $T_g$ ), and peak crystallisation temperatures ( $T_p$ 's). All runs were carried out at 25°C/min in air at temperatures below 1000°C and in dry nitrogen for any runs above 1000°C, to prevent oxidation of the high temperature head. The crucibles used were matched pairs made of platinum-rhodium alloy, and alumina was used as the reference material. Based on the procedure of Marrotta *et al.* [25], optimum nucleation studies of the glasses were carried out. Marrotta describes a method for evaluating the effectiveness of the nucleation heat treatment from the temperature of DTA/DSC crystallisation peaks. This technique may be applied to all glass systems that undergo internal crystal nucleation. Marrotta *et al.* postulated that the number of stable nuclei  $N_n$  formed in a sample per time element  $t_n$  is:

$$N_n = I t_n^b \quad (2)$$

where  $I$  is the kinetic rate constant of nucleation and  $b$  is a parameter related to the nucleation mechanism. Marrotta *et al.* also showed that if  $t_n$  is the same for each sample at each temperature  $T_N$  then the following expression applies:

$$\ln I = \frac{E_c}{R} \left[ \frac{1}{T'_p} - \frac{1}{T_p} \right] + \text{constant} \quad (3)$$

where  $E_c$  is the activation energy for crystallisation and  $R$  is the gas constant. The activation energy for crystallisation will depend on the interfacial energy between the amorphous and crystal phase. For glasses with compositions similar to the crystal phases formed, the interfacial energy, and therefore the activation for homogeneous nucleation will be reduced. A nucleation hold is expected to promote APS, thereby aiding bulk nucleation and causing a reduction in  $T_p$ , the peak crystallisation temperature.  $T'_p$  is the temperature at which

a crystallisation peak occurs after a nucleation hold and  $T_p$  is the temperature at which the latter crystallisation peak occurs without any hold. For the purposes of this study, the first crystallisation peak ( $T_{p1}$ ) corresponding to the crystallisation of fluorapatite can be taken as  $T_p$ . Nucleation holds are carried out at  $T_g$  and temperatures above in increments of typically  $10^\circ\text{C}$ .  $T_p' - T_p$  is then plotted against  $T_N$ . This gives a nucleation rate-temperature curve, which reaches a maximum at the optimum nucleation temperature. From Equations 2 and 3, Marrotta advocates the plotting of  $[1/T_p' - 1/T_p]$  against  $T_N$ . The method used here is thought to give a more accurate picture of nucleation events. Marrotta's method may show even minor fluctuations as noticeable features.

This procedure can be applied to all glass systems which undergo internal crystal nucleation. This procedure was carried out on the three ionomer glasses under investigation with hold times of 240 mins, 60 mins, 15 mins and 5 minutes. This approach could not be employed in the case of the borosilicate glass composition as it does not undergo a crystallisation process.

#### 2.4. X-ray diffraction (XRD) analysis

X-ray diffraction (XRD) was carried out on heat-treated samples of the ionomer glasses for qualitative purposes. Samples were heat-treated in the DSC at  $25^\circ\text{C}/\text{min}$  to the peak crystallisation temperatures ( $T_{p1}$  and  $T_{p2}$ ). A Philips powder diffractometer (Philips Xpert diffractometer, Philips, Eindhoven, NL) was employed using  $\text{CuK}\alpha$  x-rays.

### 3. Results and discussion

The results of the DSC and DMTA experiments are shown in Figs 2–12. DSC analysis was carried out on the Sodium-Boro-Silicate glass composition from the patent by Hammel *et al.* [22]. Fig. 2 is a DSC trace of the base glass, prior to any heat treatment.

It can be seen from Fig. 2 that there is a gradual fall-off in the curve between  $400^\circ\text{C}$  and  $700^\circ\text{C}$  but no clear evidence of a glass transition. Another sample of this glass was then heat-treated for 240 minutes at  $580^\circ\text{C}$ , in accordance with the guidelines in the patent. A DSC trace for the heat-treated glass is shown in Fig. 3.

The most obvious feature of this trace is the change in slope at  $395^\circ\text{C}$ , corresponding to the glass transition temperature. It would appear that the temperature hold has caused the glass to phase separate into two

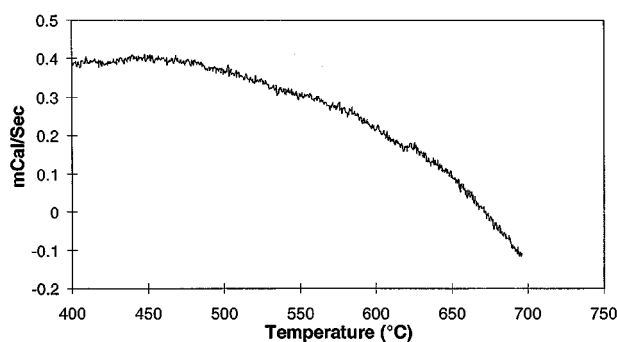


Figure 2 DSC Trace of Sodium-Boro-Silicate base glass.

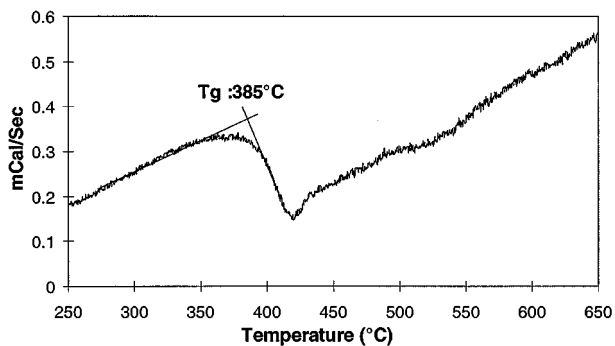


Figure 3 DSC Trace of Sodium-Boro-Silicate glass after heat-treatment at  $580^\circ\text{C}$  for 4 hours.

amorphous phases, a sodium-borate rich phase and a silica phase. The glass transition seen in Fig. 3, because of its low transition temperature is probably due to the presence of the sodium-borate rich glass phase. The glass transition of the silica glass phase would be expected at much higher temperatures.

It is worth noting that prior to any heat-treatment this glass is optically clear, but that it turns opalescent in appearance following heat-treatment. The heat treatment for 240 minutes at  $580^\circ\text{C}$  must therefore result in coarsening of an already phase separated glass structure. The failure to detect a clear glass transition temperature in the initially quenched glass may be due to the size scale of phase separation being smaller than the size scale of the parts of the glass network associated with the glass transition. Thus a composite glass transition may be expected with contributions from the  $\text{Na}_2\text{O-B}_2\text{O}_3$  rich glass phase and  $\text{SiO}_2$  glass phase. However on heating above  $580^\circ\text{C}$  further separation and coarsening will occur and any glass transition will be “washed out”. In polymer blends it has long been recognised that two immiscible polymers have to have a size  $>5\text{ nm} - 10\text{ nm}$  before two separate glass transition temperatures can be detected. A similar phenomena is likely to exist for inorganic glasses, but has not been discussed in the literature to date. DMTA analysis was also carried out on the Sodium-Boro-Silicate base glass, the results of which are shown in Fig. 4.

Fig. 4 shows a rise in  $\tan \delta$  at approximately  $395^\circ\text{C}$ . This is accompanied by a drop in the storage modulus,  $E'$ . This is due to the presence of a sodium-borate rich glass phase dispersed in a silica matrix phase and is in very good agreement with the glass transition observed

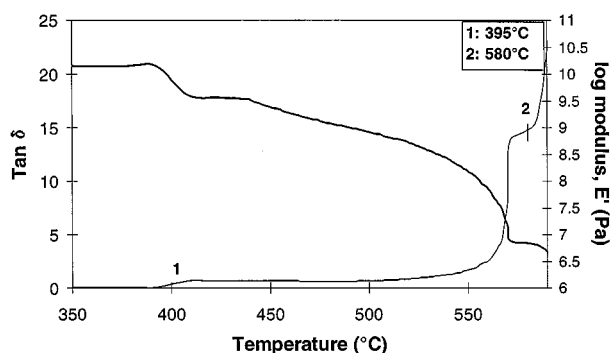


Figure 4 Storage modulus,  $E'$  (—), and  $\tan \delta$  (---) for the Sodium-Boro-Silicate base glass.

from the DSC data of the heat-treated glass. There continues to be a pronounced drop in the storage modulus by several decades, which is classical behaviour for a glass transition in organic polymers. A shoulder occurs in the second  $\tan \delta$  peak at approximately 580°C. This is the heat-treatment temperature used in the patent by Hammel *et al.* [22] and it is believed that the phase separation process is at an advanced stage at this point. The large rise in  $\tan \delta$  at approximately 600°C is believed to be the point where the glass begins to flow possibly due to melting of the sodium-borate rich phase.

DSC analysis was then conducted on ionomer glass 1, the result of which is shown in Fig. 5. A glass transition at approximately 640°C is present in Fig. 5. Two crystallisation exotherms are also present, reaching maxima at 904°C and 1082°C. There is a large temperature difference between  $T_g$  and  $T_{p1}$  for this glass. This temperature window is important in that it facilitates the casting of large homogeneous glass monoliths.

All of the ionomer glasses studied exhibited two sharp peak crystallisation temperatures. From XRD analysis the first crystallisation peak  $T_{p1}$ , can be assigned to the crystallisation of fluorapatite, while the crystallisation peak,  $T_{p2}$  corresponded to the crystallisation of mullite. Previous XRD studies by Hill and Wood [23] of glasses with Ca/P ratios between 1.25 and 2 also showed them to crystallise to fluorapatite and mullite. Fig. 6 shows the  $\tan \delta$  and  $E'$  as a function of temperature for glass 1.

There is a rise in  $\tan \delta$  at approximately 660°C. This is again typical of a glass transition and correlates with the value for  $T_g$  observed in the DSC data of Fig. 5. This rise in  $\tan \delta$  is believed to be a glass transition for a calcium-phosphate rich glass phase. A second sharper and larger loss peak is observed at approximately 742°C. This is

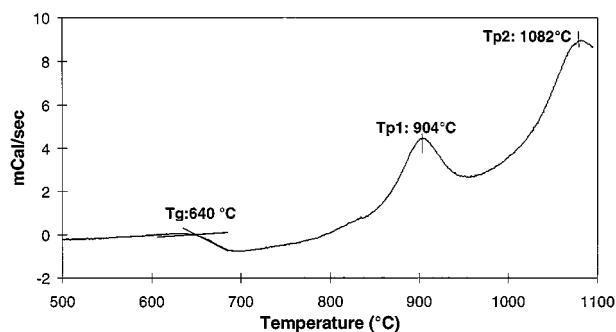


Figure 5 DSC Trace of Glass 1.

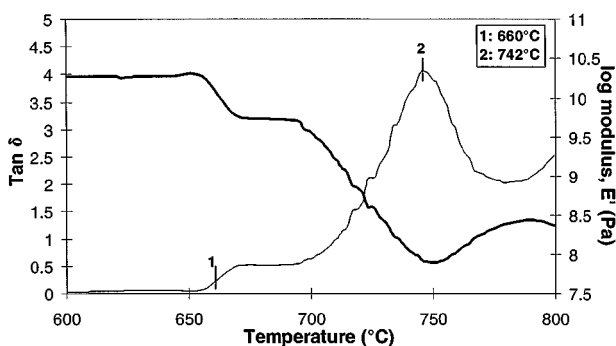


Figure 6 Storage modulus,  $E'$  (—), and  $\tan \delta$  (---) for Glass 1.

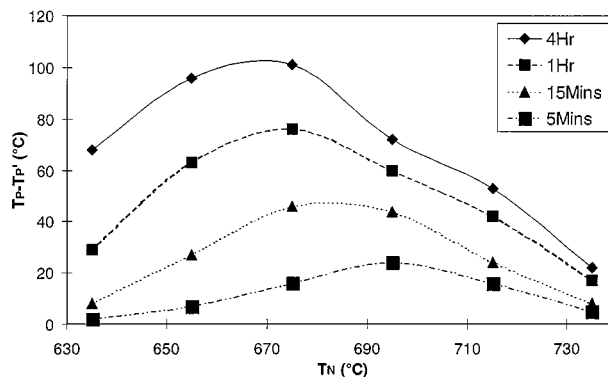


Figure 7 Optimum nucleation trace for Glass 1.

believed to be due to a second glass phase, possibly an aluminium-silicon rich glass phase. From approximately 742°C onwards a rise in  $E'$  is seen to occur corresponding to crystallisation of the glass. An optimum nucleation study for this glass was carried out in accordance with the procedure of Marrotta *et al.* [25], the results of which are shown in Fig. 7.

From Fig. 7 it can be seen that the optimum nucleation temperatures are only just above the experimentally determined glass transition temperature. The optimum nucleation temperature also moves to lower temperatures with longer hold times, consistent with a kinetically controlled APS process. For 60 minutes holds the optimum nucleation temperature is at approximately 675°C. The optimum nucleation temperature moves to lower temperatures with longer hold times suggesting that it is both a temperature and time dependent process. There is also an increase in the amplitude of the nucleation peak for longer nucleation times which shows that the longer the hold time the more pronounced its effect.

The DMTA trace of glass 2 was very similar to the DMTA trace for glass 1 which is to be expected as their compositions are very close, and again points to APS occurring and the formation of two amorphous phases. Glass bars were heated at their optimum nucleation temperatures and further DMTA runs carried out in order to assess the effect, if any of this heat treatment. A bar of glass 1 was held for 60 minutes at its optimum nucleation temperature (675°C) and DMTA was conducted. Fig. 8 shows the resulting trace.

The trace in Fig. 8 is not unlike the trace obtained for the base glass. It shows a rise in  $\tan \delta$  at approximately

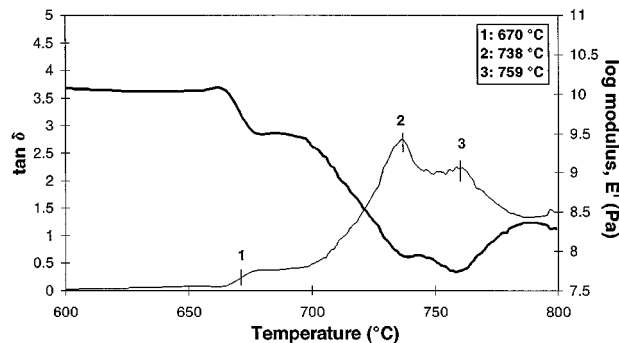


Figure 8 Glass 1, held for 1 hour at optimum nucleation temperature (660°C) Storage modulus,  $E'$  (—), and  $\tan \delta$  (---).

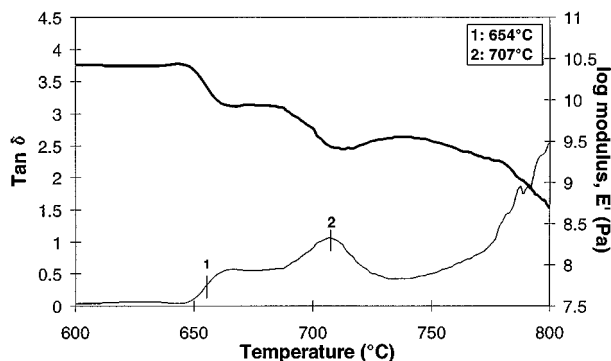


Figure 9 Storage modulus,  $E'$  (—), and  $\tan \delta$  (---) for Glass 3.

670°C and then a gradual rise to about 730°C. At this point however two peaks in  $\tan \delta$  are seen to form, in contrast to the one sharp one seen for the base glass, and there are two corresponding depressions in the storage modulus. The peaks in  $\tan \delta$  occur at 738°C and 759°C. This could point to the formation of two amorphous phases as a result of the heat-treatment and the possibility of multiple glass-in-glass phase separation. DMTA traces of this glass, having undergone 5 min, 15 min and 240 minute heat treatments were all similar to that of the base glass. None however, showed splitting of the second  $\tan \delta$  peak as in Fig. 8 above, which would suggest that the hold time of 60 minutes may be significant. It is not clear at this stage why the glass held for 240 minutes did not show splitting of the second  $\tan \delta$  peak. Fig. 9 is a DMTA trace of glass 3.

Fig. 9 shows a number of similarities and differences to the traces of glasses 1 and 2. Again there are two maxima for  $\tan \delta$ , but the amplitudes of the two maxima are a great deal lower. This could be due to the volume fractions of the two amorphous phases present being greater than for glasses 1 and 2. This could suggest that the phase separation process was already at quite an advanced stage, only the final stages of the coarsening process were picked up and there was less energy dissipated due to internal deformation. As well as this, the rise in  $\tan \delta$  at approximately 654°C is of a similar magnitude to the rise in  $\tan \delta$  for the second peak at 707°C. This is in contrast to glasses 1 and 2 where the magnitude of the rise for the second peak in  $\tan \delta$  is much larger than for the first peak. From Table I it can be seen that glass 3 has the lowest calcium fluoride content and the highest Ca/P ratio of 1.67. This will result in this glass having a less disrupted network than the other two glasses, again resulting in less internal deformation and lower amplitudes in  $\tan \delta$ . The first peak in  $\tan \delta$  is again believed to be due to a calcium-phosphate rich phase. The second peak is assumed to correspond to an aluminium-silicon rich phase but the maximum in  $\tan \delta$  corresponding to the glass transition at 707°C is quite low and would suggest that there are other components present in the aluminium-silicon rich phase.

DMTA experiments of heat-treated bars of glass 3 were conducted and yielded interesting results. Fig. 10 is a trace of glass 3 which was heated for 15 minutes at its optimum nucleation temperature. This trace is similar to that of the base glass in that it exhibits two peaks for  $\tan \delta$  at the same temperatures as the base

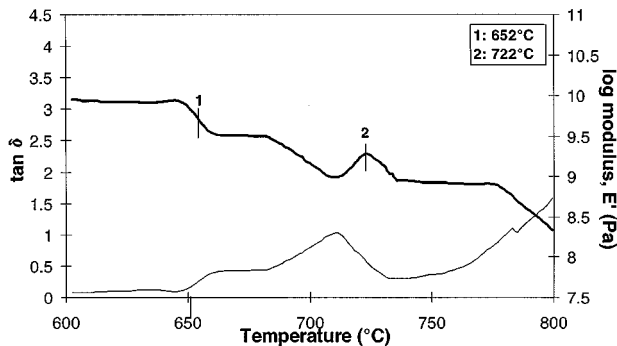


Figure 10 Glass 3, held for 15 minutes at optimum nucleation temperature (655°C) Storage modulus,  $E'$  (—), and  $\tan \delta$  (---).

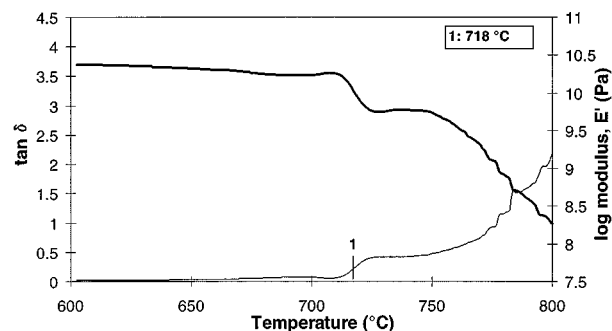


Figure 11 Glass 3, held for 1 hour at optimum nucleation temperature (655°C) Storage modulus,  $E'$  (—), and  $\tan \delta$  (---).

glass. There is a gradual fall-off in the storage modulus, but also an unusually sharp peak in  $E'$  at 722°C which was much broader for the base glass. This is the only feature which suggests that the heat treatment is having any effect and distinguishes the heat-treated glass from the base glass.

A further experiment was conducted on glass 3, which had been held for 60 minutes at its optimum nucleation temperature, the results of which are shown in Fig. 11. Fig. 11 is markedly different to the previous two traces. There is only one rise in  $\tan \delta$ , occurring at approximately 718°C, which was the position of the second maximum in  $\tan \delta$  for the base glass. This could be as a result of the lower glass transition temperature calcium-phosphate rich glass phase having crystallised. A sample of glass 3 heat treated for 240 minutes at its optimum nucleation temperature was almost identical to Fig. 11. It would therefore appear that the heat treatments are having an effect with a critical heat treatment time occurring between 15 minutes and 60 minutes.

An optimum nucleation study was conducted on this glass the results of which are presented in Fig. 12. The most obvious feature of Fig. 12 is the amplitudes of the optimum nucleation peaks. There is little difference in the amplitudes of the peaks for the 240 min, 60 min, 15 min and 5 minute holds. The amplitude of the peak for the glass held for 5 minutes is very pronounced which would appear to indicate that even very small hold times are promoting amorphous phase separation and bulk nucleation. There is therefore less time required to promote the transformation from amorphous phase to crystal nucleation, with even a hold time of just 5 minutes having a marked effect on the crystallisation behaviour.

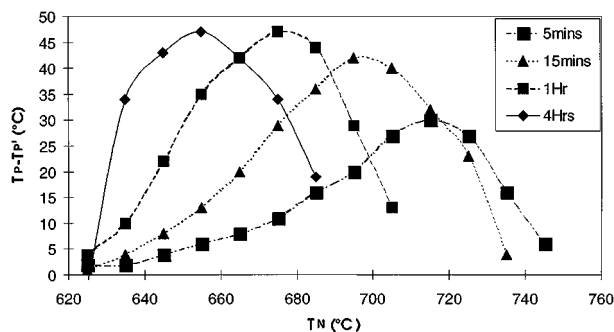


Figure 12 Optimum nucleation trace for Glass 3.

The nucleation data agrees with the DMTA results for this glass which exhibited rises in  $\tan \delta$  of lower amplitude, indicating that the formation of the two amorphous phases was perhaps occurring with greater ease, or took less time for completion than for glasses 1 and 2.  $\tan \delta$ , which is sometimes referred to as the internal friction, will increase as internal deformation occurs and energy is dissipated as heat. Glass 3 has the fluorapatite Ca/P ratio of 1.67 and has a similar composition to the apatite ( $\text{Ca}_5(\text{PO}_4)_3\text{F}$ ) crystal phase formed, thus reducing interfacial energy and therefore the activation energy for homogeneous nucleation [26]. It is assumed that these glasses have phase separated from the melt, the extent of this is unknown but some are expected to be in a more advanced stage of separation than others. It is reasonable to assume that Glass 3 may be at a more advanced stage of phase coarsening on pouring from the melt, as its composition is more favourable for APS. It could be therefore that much of the separation process has already occurred and that even short time periods are strongly influencing the nucleation events, as seen in Fig. 12.

#### 4. Conclusions

High temperature dynamic mechanical thermal analysis was shown to be a valuable technique for studying structural changes in both ionomer glasses and a sodium-boro-silicate glass. High temperature DMTA accurately determined two glass transition temperatures for each of the glasses studied, something which was impossible to do with DSC alone. DMTA traces of two ionomer glasses of the same series and of similar composition were in good agreement. A sodium-boro-silicate glass, which is well known in the literature to undergo APS was shown to have two glass transition temperatures, the first of which was due to a sodium-borate rich phase. The results, when compared with those for the ionomer glasses studied, support the view that crystal nucleation is via prior amorphous phase separation in ionomer glasses. The three ionomer glasses studied exhibited dome shaped optimum nucleation curves with maxima just above the glass transition temperature. The ability to self nucleate

and to undergo nucleation only slightly above the glass transition temperature is also indicative of a nucleation mechanism involving prior amorphous phase separation. The peaks of the nucleation curves shifted to lower temperatures with longer hold times indicating the time dependency of the APS process.

#### Acknowledgements

The authors would like to gratefully acknowledge the support of Brite EuRam Contract BRPR-CT96-0230. The authors would also like to offer thanks to Mr. Nigel Bubb for his technical assistance with the DMTA instrument.

#### References

1. W. VOGEL, in "Chemistry of Glass," (The American Ceramic Society Inc. Columbus, OH, 1985) p. 69.
2. N. FORD and R. TODHUNTER, in "Glasses and Glass Ceramics," (Chapman and Hall, 1989) p. 203.
3. Z. STRNAD, in "Glass-Ceramic Materials," (Elsevier Science Publishing Company Inc. Amsterdam, 1986) p. 31.
4. P. F. JAMES, in "Glasses and Glass-Ceramics," (Chapman and Hall, London, 1989) p. 91.
5. *Idem.*, *J. Mater. Sci.* **10** (1975) 1802.
6. S. CRISP and A. D. WILSON, *J. Dent. Res.* **53** (1974) 1408.
7. D. G. GROSSMAN, in "Advances in Ceramics, Vol. 4," (American Ceramic Society, Ohio, 1982) p. 252.
8. P. J. ADAIR and D. G. GROSSMAN, *Int. J. Periodont. Rest. Dent.* **2** (1984) 33.
9. A. CLIFFORD and R. HILL, *J. Non-Cryst. Solids.* **2372** (1995) 1.
10. R. H. DOREMUS, in "Glass Science," (John Wiley and Sons Ltd., USA, 1973) p. 80.
11. P. W. McMILLAN, in "Glass Ceramics," (Academic Press, London, 1979) p. 76.
12. M. TOMOZOWA, in "Advances in Nucleation and Crystallisation in Glasses," (American Ceramic Society, 1971) p. 41.
13. T. I. BARRY, D. J. CLINTON and A. D. WILSON, *J. Dent. Res.* **58** (1979) 1072.
14. R. G. HILL and A. D. WILSON, *Glass Tech.* **29**(4) (1988) 150.
15. D. E. RAY, in "Amorphous Materials," (Wiley-Interscience, New York, 1972) p. 39.
16. R. W. DOUGLAS, P. J. DUKE and O. V. MAZURIN, *Phys. Chem. Glasses* **9** (1968) 169.
17. J. M. STEVELS, *J. Non-cryst. Solids* **73** (1985) 165.
18. G. M. BARTENER, *Wiss. Z.-Friedrich Schiller Univ. Jena, Math.-Naturwiss. Reihe.* **32** (1983) 385.
19. J. J. MILLS, *J. Non-Cryst. Solids* **14** (1974) 255.
20. J. PEREZ, B. DUPERRAYARD and D. LEFEVRE, *ibid.* **44** (1981) 113.
21. R. HILL and P. GILBERT, *J. Am. Ceram. Soc.* **76**(2) 25 (1993) 417.
22. J. HAMMEL and T. ALLERSMO, US Patent, No. 3,972,721 (August 3, 1976).
23. D. WOOD and R. HILL, *Clin. Mater.* **7** (1991) 301.
24. R. HILL and D. WOOD, *J. Mater. Sci. Mats. in Med.* **6** (1995) 311.
25. A. MARROTTA, A. BURI, F. BRANDA and S. SAIELLO, in "Advances in Ceramics, Vol. 4," (The American Ceramic Society, Inc. 1982) p. 146.
26. E. D. ZANOTTO and E. MÜLLER, in "The Physics of Non-Crystalline Solids," (Taylor and Francis Ltd. 1992) p. 387.

Received 3 June 1999

and accepted 3 February 2000